Molecular Mechanisms Underlying Ionic Remodeling in a Dog Model of Atrial Fibrillation

Lixia Yue, Peter Melnyk, Rania Gaspo, Zhiguo Wang, Stanley Nattel

Abstract—The rapid atrial rate during atrial fibrillation (AF) decreases the ionic current density of transient outward K^+ current, L-type Ca^{2+} current, and Na^+ current, thereby altering cardiac electrophysiology and promoting arrhythmia maintenance. To assess possible underlying changes in cardiac gene expression, we applied competitive reverse transcriptase–polymerase chain reaction to quantify mRNA concentrations in dogs subjected to 7 (group P7 dogs) or 42 (group P42 dogs) days of atrial pacing at 400 bpm and in sham controls. Rapid pacing reduced mRNA concentrations of Kv4.3 (putative gene encoding transient outward K^+ current; by 60% in P7 and 74% in P42 dogs; $P<0.01$ and $P<0.001$, respectively, versus shams), the α_{1c} subunit of L-type Ca^{2+} channels (by 57% in P7 and 72% in P42 dogs; $P<0.01$ versus shams for each) and the α subunit of cardiac Na^+ channels (by 18% in P7 and 42% in P42; $P=$NS and $P<0.01$, respectively, versus shams) genes. The observed changes in ion channel mRNA concentrations paralleled previously measured changes in corresponding atrial ionic current densities. Atrial tachycardia did not affect mRNA concentrations of genes encoding delayed or Kir2.1 inward rectifier K^+ currents (of which the densities are unchanged by atrial tachycardia) or of the Na^+,Ca^{2+} exchanger. Western blot techniques were used to quantify protein expression for Kv4.3 and Na^+ channel α subunits, which were decreased by 72% and 47%, respectively, in P42 dogs ($P<0.001$ versus control for each), in a manner quantitatively similar to measured changes in mRNA and currents, whereas Na^+,Ca^{2+} exchanger protein concentration was unchanged. We conclude that chronic atrial tachycardia alters atrial ion channel gene expression, thereby altering ionic currents in a fashion that promotes the occurrence of AF. These observations provide a potential molecular basis for the self-perpetuating nature of AF. **(*Circ Res*. 1999;84:776-784.)**

Key Words: arrhythmia, cardiac ■ molecular biology ■ channels, ion ■ remodeling, atrial ■ Ca^{2+} ■ K^+

Alterations in gene expression are important in a wide variety of disease processes.[1] Pathological perturbations of physiological function can cause changes in gene expression that lead to secondary abnormalities that contribute to the phenotypic manifestations and progression of disease.[2–4] Atrial fibrillation (AF) is the most common cardiac arrhythmia in clinical practice and can lead to potentially serious clinical consequences, including thromboembolism, impaired physical capacity, reduced left ventricular function, and stroke.[5] The treatment of AF remains suboptimal because of limited efficacy and potential side effects of drug therapy.[6] Recent research indicates that one important potential element in the resistance of AF to treatment is the tendency of the arrhythmia to alter the properties of the heart in a way that promotes AF maintenance.[7,8] The rapid atrial rate appears to be the central factor in the electrophysiological changes produced by AF.[9] Chronic atrial tachycardia at a rate (400 bpm) in the range of that of AF produces important alterations in ion channel function (reduced densities of transient outward K^+ current [I_{to}], L-type Ca^{2+} current [I_{Ca}], and Na^+ current [I_{Na}]) that result in a functional substrate that supports the maintenance of AF.[7,10–13] The molecular mechanisms that cause these changes in ion channel function are unknown. Over the past several years, considerable progress has been made in identifying the molecular composition of the principal subunits of cardiac ion channels. The sequences encoding pore-containing subunits of cardiac I_{Ca},[14,15] I_{Na},[16] and I_{to}[17,18] in mammalian systems have been described, as have sequences encoding components of 2 currents, the inward rectifier[19] and rapid delayed rectifier[20,21] K^+ currents (I_{K1} and I_{Kr}, respectively), that are not altered by atrial tachycardia.[10] The present studies were designed to quantify mRNA concentrations corresponding to pore-containing subunits of 5 cardiac ion channels (I_{to}, I_{Na}, I_{Ca}, I_{K1}, and I_{Kr}) in atrial tissue from dogs subjected to 7 and 42 days of rapid atrial pacing (P7 and P42 dogs, respectively), and to compare the results with measurements obtained in sham-instrumented dogs (P0 dogs) and previously determined alterations in ion current density. In addition, Western blot studies were performed to quantify changes in membrane protein content of 2 molecular species

Received August 26, 1998; accepted January 24, 1999.

From the Department of Pharmacology and Therapeutics (L.Y., S.N.) and the Department of Pathology (P.M.), McGill University; the Department of Medicine (R.G., Z.W., S.N.), University of Montreal; and the Research Center (L.Y., P.M., R.G., Z.W., S.N.), Montreal Heart Institute, Montreal, Quebec, Canada.

Correspondence to Stanley Nattel, MD, Research Center, Montreal Heart Institute, 5000 Bélanger Street East, Montreal, Quebec, H1T 1C8, Canada. E-mail nattel@icm.umontreal.ca

Circulation Research **is available at http://www.circresaha.org**

(I_{to} and I_{Na}) for which significant changes in mRNA concentration were detected.

Materials and Methods

Preparation of the Dog Model

We used a previously described approach to implant pacemakers in subcutaneous pockets in the necks of 15 mongrel dogs.[10–12] After 24 hours of recovery, 10 dogs were subjected to continuous right atrial pacing at 400 bpm for 7 or 42 days (n=5 for each group). Five dogs in which the pacemaker was not activated served as the P0 (sham control) group. On the study day, dogs were anesthetized with morphine 2 mg/kg and α-chloralose 120 mg/kg and a right thoracotomy was performed. AF was induced by burst atrial pacing with 4× threshold 4-ms pulses at 10 Hz. Mean±SEM AF duration was 8.4±3.0 s for P0 dogs, 1522±563 s for P7 dogs ($P<0.05$ versus P0 dogs) and 2700±0 s (AF sustained in all) for P42 dogs ($P<0.001$ versus P0 dogs), which confirmed the arrhythmogenic alterations caused by rapid atrial pacing. After AF duration measurement, the right atrium was removed, frozen in liquid nitrogen and stored at −80°C.

RNA Preparation

Total RNA was isolated from frozen pectinate muscle tissue of right atria. In brief, 1 g of tissue was homogenized in 10 mL of Trizol reagent (Gibco BRL) extracted with chloroform and precipitated in isopropyl alcohol. Total RNA was incubated in DNase I (0.1 U/μL, Ambion) for 15 minutes, extracted by use of phenol-chloroform, precipitated in isopropyl alcohol, and subsequently dissolved in diethylpyrocarbonate-treated water. The amount of total RNA was determined spectrophotometrically (Spectronic Genesys) at a wavelength of 260 nm, and the RNA was stored at −80°C for later analysis. mRNA was purified with the Poly(A) Quik mRNA isolation system (Stratagene). The integrity of each sample was confirmed by analysis on a denaturing agarose gel.

Cloning of cDNA Fragments of Ion Channels From Dog Atrium and Designing of Gene-Specific Primers

The principle of competitive polymerase chain reaction (PCR) involves amplification in a truly competitive fashion, because the internal standard (mimic) and the target sequences compete for the same primer and, therefore, for amplification. It is thus important to design gene-specific rather than degenerate primers. We therefore cloned partial cDNA sequences of the α_1 subunit of the cardiac Ca^{2+} channel, the α subunit of the Na^+ channel, the Kv4.3 α subunit, canine Kir2.1 (DIRK), the canine counterpart of HERG (DERG), and the Na^+,Ca^{2+} exchanger (NCX) from canine atrial tissue samples. Degenerate primers for reverse transcription (RT)–PCR were designed on the basis of published sequences.[14–22] The specificity of the primers was confirmed with the basic local alignment search tool (BLAST).[23] PCR products were size-separated on 1.5% agarose gels. Bands of desired size were purified with the Glassmax DNA Isolation Spin Cartridge System (Gibco BRL). The purified DNA fragments were subcloned into pGEM-T easy vector (Promega). Sequences of all constructs were analyzed with Sequenase version 2.0 (Amersham).

Synthesis of RNA Internal Standards

Synthetic RNA internal standards (mimics) were manufactured with the procedure shown in Figure 1. Gene-specific primers for RT-PCR (Table) were designed without degeneracy according to the obtained sequences and their specificity confirmed by BLAST and the FASTA program for rapid comparison of nucleotide sequences. A 392-bp fragment of α-actin was synthesized from the region of 111 to 502 using the primers shown in the Table. The 392-bp PCR product was purified on an agarose gel and its sequence confirmed. The defined product was used to construct an internal standard for the α_{1c} subunit of the L-type Ca^{2+} channel, DERG, and the Na^+ channel α subunit. Similar methods were used to construct internal standards for the Kv4.3 potassium channel α subunit, NCX, and DIRK with the use of a 460-bp fragment of human α-actin.

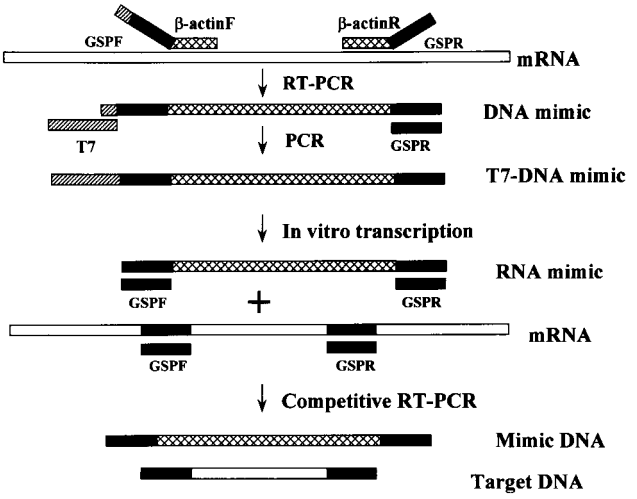

Figure 1. Schematic diagram indicating procedures used to obtain RNA mimic (internal standard) and to perform competitive RT-PCR. GSPF and GSPR indicate forward and reverse gene-specific primers, respectively; β-actinF and β-actinR, forward and reverse primers, respectively, for β-actin sequence; and T7, T7 promoter sequence. For details, see text.

First-strand cDNA was synthesized by RT with canine atrial mRNA and random primers. Chimeric primer pairs were constructed by appending gene-specific primers at the 5′- end of α- (β-)actin primers, and an 8-nucleotide (GGCCGCGG) linker homologous to the 3′- end of the T7 promoter sequence was conjugated to the 5′-end of each gene-specific sense primer. The chimeric primers were used in a PCR reaction (*Taq* polymerase; annealing temperature, 54°C) with the first-strand DNA to generate an actin cDNA sequence flanked by gene-specific primers, with the short T7 promoter sequence at the 5′- end. The product of this PCR was diluted 50-fold, and 1 μL was used as a template in a second PCR. Primers used in the second PCR included a T7 promoter primer (sense) and a gene-specific anti-sense primer, and PCR was performed at annealing temperature of 60°C. The resulting product, carrying the T7 promoter, gene-specific primers, and an internal α- or β-actin fragment was gel-purified (Glassmax DNA Isolation Spin Cartridge System, Gibco BRL) and used as a template for in vitro transcription. In vitro transcription was conducted with *mMESSAGE mMACHINE* (Ambion) at 37°C for 1 hour. RNase-free DNase I (1 μL of 2 U/μL solution) was added to a 20-μL reaction mixture, which was then incubated at 37°C for 15 minutes. The RNA formed was extracted with phenol chloroform and precipitated with ethanol. The RNA pellet was dried and dissolved in RNAse-free water, the quantity of RNA was determined by spectrophotometry and gel analysis, and the sample was stored at −80°C for later use.

Competitive RT-PCR

Serial dilutions of the RNA internal standards were added to 100 ng of sample mRNA in a series of reaction mixtures. Sample mRNA and RNA internal standards were denatured at 65°C for 15 minutes and chilled on ice for 5 minutes before being added to the reaction mixture. RT was conducted at 25°C for 10 minutes and 42°C for 60 minutes with a 20-μL first-strand cDNA synthesis mixture (3.2 μg of random hexamers, 1 mmol/L deoxynucleotide mixture (dNTP), 50 U of RNase inhibitor, 20 U of AMV reverse transcriptase). Aliquots of first-strand cDNA (10 μL) were amplified by PCR in a 50-μL solution containing (mmol/L) Tris-HCl 10 (pH 8.3), KCl 50, dNTP 0.8, and $MgCl_2$ 1.5 as well as 2.6 U *Taq* polymerase and 0.2 μmol/L gene-specific primers. The reaction mixture was denatured (94°C for 3 minutes), run for 30 cycles of 94°C denaturing for 30 seconds, annealed at the appropriate temperature (Table) for 45 seconds, and

Conditions Used for Competitive PCR

	Sense/Antisense Primer	Bases Spanned, bp	Product Size, bp	Tm, °C	Reference No.
I_{Na}	TGCATTAACCAGACAGAGG/CCAATAAAGAGGTTCAGGGTG	4237–4550	314	54	16
I_{Ca}	ATCATCATCTACGCCATCATCGG/ATCCAGTATAGTACGTCAGTCC	761–1041	281	54	14, 15
Kv4.3	TAGATGAGCAGATGTTTGAGC/ACTGCCCTGGATGTGGATG	1533–1744	212	54	17
DIRK	GACCTGGAGACGGACGAC/AGCCTGGAGTCTGTCAAAGTC	910–1302	393	52	19
DERG	ACGGCGCTCTACTTCACC/ACCGCGTTCATGTCGATG	2020–2330	311	52	20
NCX	TTGAGATTGGAGAGCCCC/CTCCTCCTCTTTGCTGGTC	1889–2100	212	52	21
β-actin	CAGAGCAAGAGGGGCATC/AGGTAGTCGGTCAGGTCC	111–502	392	54	...*
α-actin	ACCGGGAGAAGATGACTCAG/AATGAAGGAGGGCTGGAAG	329–1583†	460	54	...*
T7 promoter	AGAATTCTAATACGACTCACTATAGGGCCGCGC				

*Sequences obtained from GenBank; accession numbers Z70044 (β-actin) and J00070 (α-actin).

†The product is generated from exons in the 329- to 1583-bp region.

The NCX clone we obtained was identical to the sequence (Reference 21) previously published for dog atrium.

elongated at 72°C for 1 minute, with a final extension period of 10 minutes at 72°C.

Electrophoresis of the amplified products was performed on 1.5% to 2% agarose gels containing Tris acetate 40 mmol/L, EDTA 1 mmol/L, and ethidium bromide. Ethidium bromide fluorescence images were captured with a Nighthawk camera under ultraviolet light, and the density of each band was determined by use of Quantity One software. A DNA mass ladder was used to construct a standard curve to quantify the intensity of PCR product bands. The logarithm of the ratio of internal standard to target intensity (corrected for molecular weight) for each reaction tube was plotted as a function of the logarithm of RNA internal standard concentration. The resulting points were fitted by linear regression to determine the point of identity.

The absence of genomic contamination in the mRNA samples and the absence of cDNA contamination in the RNA internal standards were confirmed by the absence of a signal for reverse transcriptase–negative controls. To assure equal amplification of sample mRNA and RNA internal standards, known quantities of target and mimic RNA were coamplified in single-reaction tubes. In all cases, the target sequence and its corresponding mimics were amplified with similar efficiencies (see Figure 2). The equivalence of sample mRNA input in each experiment was established by spectrophotometry and noncompetitive PCR for the actin internal standard.

Western Blot Studies

Membrane preparations were obtained as previously described[24] by a modification of the protease inhibitors. Specifically, pepstatin 1 μg/mL, leupeptin 1 μg/mL, aprotinin 2 μg/mL, benzamidine 0.1 mg/mL, calpain inhibitors I and II (8 μg/mL each), and 4-(2-aminoethyl)-benzenesulfonyl-fluoride hydrochloride (Pefabloc SC) (0.5 mmol/L) were included in the Tris/EDTA solution (10 mmol/L Tris-base, 1 mmol/L EDTA) that contained the tissue samples. All protease inhibitors were obtained from Sigma Chemical Co except for Pefabloc SC (Boehringer Mannheim). All procedures were performed on ice, the centrifuge rotor was precooled, and centrifugation was performed at 4°C.

The solubilized membrane proteins (45 μg) were fractionated on 8% SDS-polyacrylamide gels. The proteins were then transferred electrophoretically to Immobilon-P polyvinylidene fluoride membranes (Millipore) in 25 mmol/L Tris-base, 192 mmol/L glycine, and 5% methanol at 0.07A for 18 hours. The membranes were blocked using 5% nonfat dry milk (Bio-Rad) in TBS (Tris-HCl 50 mmol/L, NaCl 500 mmol/L; pH 7.5) containing 0.05% Tween-20 (TTBS) for 2 hours at room temperature. Membranes were then incubated overnight in primary antibody solutions in 1% nonfat dry milk in TTBS. The primary antibody against the α subunit of the Na^+ channel (Alomone Labs) was used at a dilution of 1:150, the anti-Kv4.3 antibody at a dilution of 1:375, and NCX antibody (Research Diagnostics) at 1:750. Attempts were made to image the α_{1c} subunit of the L-type Ca^{2+} channel with an antibody from Alomone Labs; however, because of a low signal-to-noise ratio, these attempts were unsuccessful. After overnight incubation, the membranes were washed 3 times in TTBS and reblocked in 1% nonfat dry milk in TTBS for 10 minutes. They were incubated with horseradish peroxidase–conjugated anti-rabbit IgG (1:5000) in 5% nonfat dry milk in TTBS for 30 minutes and washed in TTBS 4 more times. Antibody detection was performed with Western blot chemiluminescence reagent plus (NEN Life Science Products).

The density of bands on Western blots was quantified by use of a scanner (PDI 420oe) and Quantity One software (PDI), which included a background subtraction algorithm. To confirm equal protein loading, the densities of nonspecific bands in the ≅90 kDa

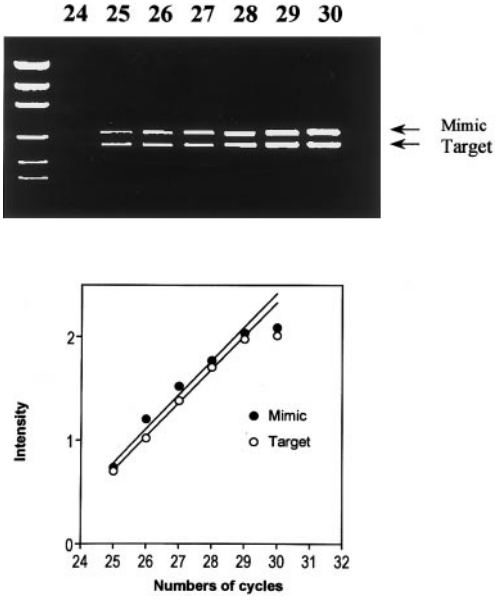

Figure 2. Kinetics of amplification of DERG internal standard and DERG fragments. Constant amounts of RNA internal standard and DERG mRNA (2 pg each) were amplified in a single reaction tube with DERG primers. After 24 amplification cycles and after each of 5 additional cycles, a 10-μL aliquot of reaction mixture was removed and the products resolved on agarose gel (upper panel). The relative intensities of the bands corresponding to internal standard and DERG products were quantified by computer imaging. The intensities of specific amplified products (circles) were plotted as a function of the number of cycles (lower panel). Similar studies were performed for all constructs to confirm equal amplification of internal standards and targets.

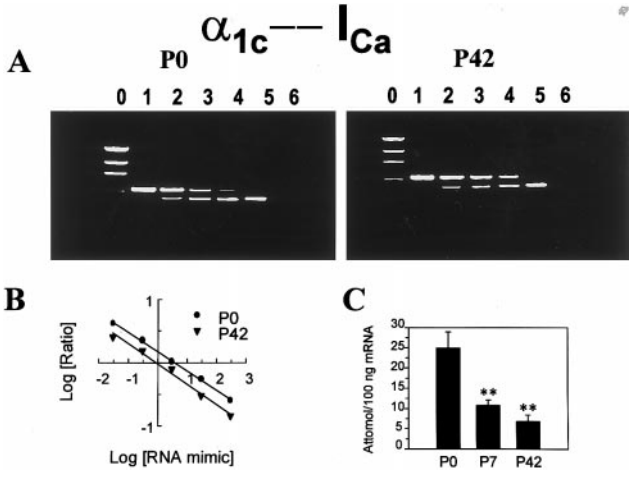

Figure 3. A, Representative agarose gels for competitive RT-PCR of the α_{1c} subunit of I_{Ca} in tissue from P0 and P42 hearts. Lane 0 shows DNA mass ladder; lanes 1 to 5, results obtained with serial dilutions of RNA internal standard (lane 1, 300 pg; lane 2, 30 pg; lane 3, 3 pg; lane 4, 0.3 pg; and lane 5, 0.03 pg); lane 6, reverse transcriptase–negative control. Lower bands correspond to channel mRNA; upper bands are internal standards. B, Abundance of α subunit of Ca^{2+} channel mRNA was determined from a graph of the logarithmic ratio of optical intensity of amplified target DNA/mimic DNA versus logarithm of mimic RNA concentration. C, Mean±SEM abundance of I_{Ca} α subunit mRNA from P0, P7, and P42 dogs (n=5 analyses from 1 heart each per group; $^{**}P<0.01$ vs P0 dogs).

region (for the Na^+ channel) and the ≅45 kDa region (for Kv4.3) were compared. All gels contained membrane preparations for each of several P42 and several P0 hearts to exclude artifacts due to intergel differences in density and background.

Statistical Analysis

Group data are expressed as mean±SEM. Group comparisons were performed with ANOVA. If significant differences were indicated by ANOVA, a *t* test with Bonferroni's correction was used to evaluate differences between individual mean values. A 2-tailed $P<0.05$ was taken to indicate statistical significance.

Results

Canine cDNA Clones

Partial cDNA sequences were cloned from dog atrium for the α_{1c} subunit of the L-type Ca^{2+} channel (281 bp, GenBank accession No. AF048752); Kv4.3 (212 bp, No. AF049887); the α subunit of the Na^+ channel (314 bp, No. AF017428); canine atrial Kir2.1, DIRK (378 bp, No. AF048751); and DERG (311 bp, No. AF017429). The sequences show substantial homology with analogous clones from other species[14–20] (87% to 94% at the nucleotide level and 94% to 100% at the amino acid level).

Expression of mRNA for the α_{1c} Subunit of the L-Type Ca^{2+} Channel

Figure 3A shows representative gels from the competitive RT-PCR of the L-type Ca^{2+} channel α_{1c} subunit. Lane 0 is a DNA mass marker, and lanes 1, 2, 3, 4, and 5 were obtained by the addition of 300, 30, 3, 0.3, and 0.03 pg of the RNA internal standard, respectively, along with 100 ng of mRNA extracted from the atrium of a P0 dog (left) and a P42 dog (right). The lower band in each lane corresponds to the Ca^{2+} channel mRNA product, and the upper band is the internal standard signal. The sixth lane was obtained with an initial reaction tube containing 300 pg of RNA internal standard and 100 ng of sample mRNA, without the addition of reverse transcriptase. Internal standard and sample mRNA bands have similar intensity in lane 3 for the P0 dog, whereas for the P42 dog the point of equivalence is in lane 4, corresponding to a substantially lower I_{Ca} mRNA concentration. Figure 3B shows the relations between relative intensities of internal standard and gene-specific bands as a function of the quantity of RNA internal standard for the gels in panel A. The intersection of regression lines with the horizontal axis shifts to the left in the paced dog, which indicates a substantial reduction in gene-specific mRNA. Figure 3C shows the mean±SEM Ca^{2+} channel subunit mRNA concentration in 5 hearts (1 independent determination per heart) from each group of dogs, which decreased significantly within 7 days.

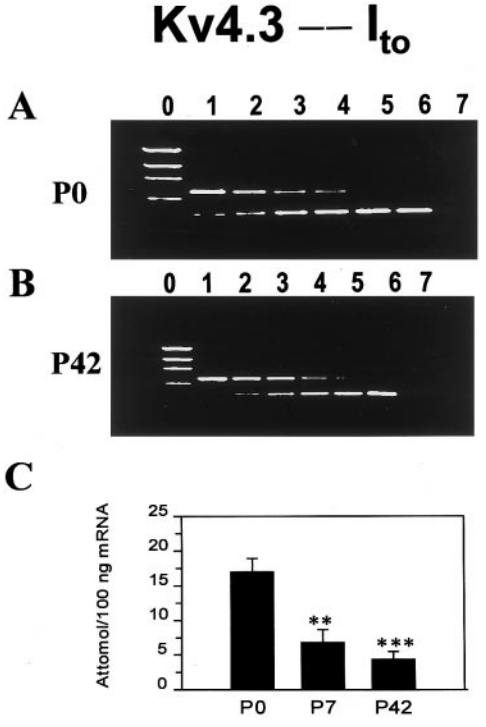

Figure 4. Agarose gels for competitive RT-PCR of Kv4.3 K^+ channel subunits in tissue from sham (A) and P42 (B) hearts. Lane 0 shows DNA mass ladder; lanes 1 to 6, results obtained with serial dilutions of RNA internal standard (lane 1, 20 pg; lane 2, 2 pg; lane 3, 0.2 pg; lane 4, 0.02 pg; lane 5, 0.002 pg; and lane 6, 0.0002 pg); lane 7, reverse transcriptase–negative control. Lower bands correspond to channel mRNA; upper bands are internal standards. C, Mean±SEM Kv4.3 mRNA concentration in right atria from P0, P7, and P42 dogs (n=5 analyses, 1 analysis per heart per group; $^{**}P<0.01$, $^{***}P<0.001$ vs P0 dogs).

Expression of Kv4.3 Subunit mRNA

Figure 4A shows gels obtained by competitive PCR for the Kv4.3 K^+ channel subunit in a P0 heart. Lanes 1, 2, 3, 4, 5, and 6 are from initial reaction mixtures containing 20, 2, 0.2, 0.02, 0.002, and 0.0002 pg, respectively, of the RNA internal standard for Kv4.3. Lane 7 was obtained with 20 pg of the internal standard and 100 ng of mRNA without the use of reverse transcriptase. As for the Ca^{2+} channel, the point of

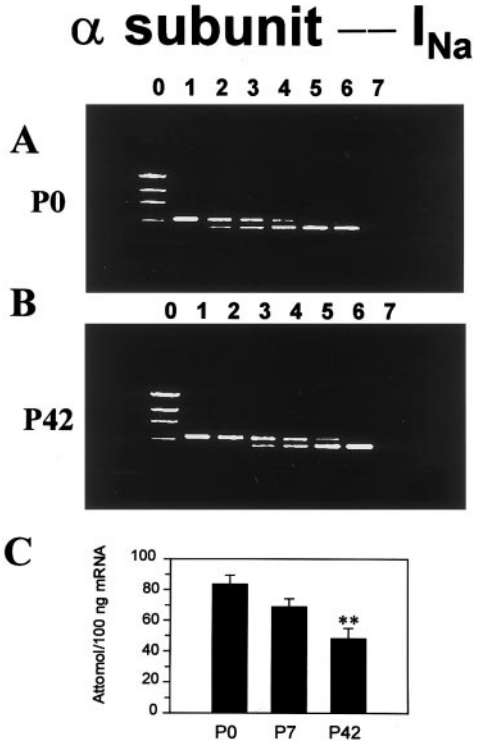

Figure 5. Agarose gels for competitive RT-PCR of the α subunit of I_{Na} in tissue from sham (A) and P42 (B) hearts. Lane 0 shows DNA mass ladder; lanes 1 to 6, results obtained with serial dilutions of RNA internal standard (lane 1, 100 pg; lane 2, 10 pg; lane 3, 2 pg; lane 4, 0.4 pg; lane 5, 0.08 pg; and lane 6, 0.016 pg); lane 7, reverse transcriptase–negative control with 100 pg of RNA internal standard. Lower bands correspond to channel mRNA products; upper bands to internal standards. C, Mean±SEM abundance of Na^+ channel α subunit mRNA from P0, P7, and P42 dogs (n=5 analyses for each group; $^{**}P<0.01$ vs P0 dogs).

equivalence between mimic and gene-specific mRNA bands moves to the right in the P42 dog (Figure 4B), which indicates a decrease in mRNA concentration. Mean data for 5 hearts in each group are shown in Figure 4C and indicate a progressive decrease in Kv4.3 mRNA concentration in paced dogs.

Expression of Cardiac Na^+ Channel α Subunit mRNA

Figure 5 shows results for the cardiac Na^+ channel α subunit from a P0 (Figure 5A) and a P42 (Figure 5B) dog. RNA internal standard quantities in the reaction mixture for lanes 1, 2, 3, 4, 5, and 6 of Figure 4A were 100, 10, 2, 0.4, 0.08, and 0.016 pg, respectively. The equivalent point is shifted to the right in the paced dog, which indicates decreased mRNA concentrations. Figure 5C shows mean mRNA concentrations from 5 hearts in each group. A slight, nonsignificant reduction was noted after 7 days of pacing, and a significant reduction was noted after 42 days.

Expression of DIRK, DERG, and NCX Transcripts

The above data are for clones believed to play a role in I_{Ca}, I_{to}, and I_{Na}, 3 channels that we have found to be altered significantly in the rapid-pacing AF model.[10,11] To evaluate mRNA concentrations corresponding to other ion transport mechanisms, we measured the concentration of mRNA for DIRK, DERG, and NCX, clones that correspond to the inward rectifier I_{K1}, the rapid delayed rectifier I_{Kr}, and NCX, respectively (Figure 6). There were no changes in the point of equivalence between gene-specific signals and internal standards in paced dogs. Overall, mRNA concentrations averaged 64.5±6.7 and 61.5±5.7 amol per 100 ng mRNA in 5 P0 and 5 P42 hearts, respectively (P=NS), for DIRK; 30.0±7.1 and 30.8±8.2 amol per 100 ng mRNA in 5 P0 and 5 P42 hearts, respectively (P=NS), for DERG; and 128.8±40.2 and 137.2±31.2 amol per 100 ng mRNA in 5 P0 and 5 P42 hearts, respectively (P=NS), for NCX.

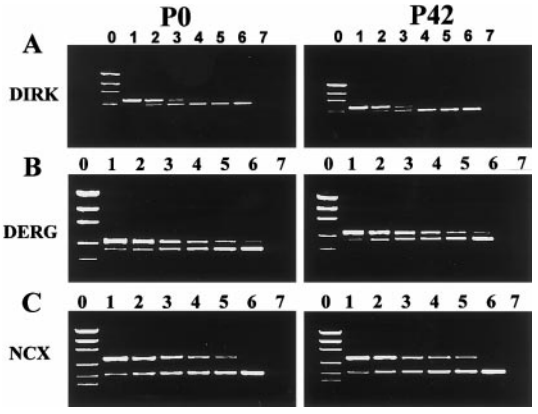

Figure 6. Representative gels from competitive RT-PCR analyses for DIRK (A), DERG (B), and NCX (C) mRNA level in sham (P0) and paced (P42) dogs. A, Lane 0 shows DNA mass ladder; lanes 1 to 6, serial dilutions of DIRK RNA internal standard (lane 1, 100 pg; lane 2, 10 pg; lane 3, 1 pg; lane 4, 0.2 pg; lane 5, 0.1 pg; and lane 6, 0.02 pg); lane 7, reverse transcriptase–negative control. B, Lane 0 shows DNA mass ladder; lanes 1 to 6, serial dilutions of DERG RNA internal standard (lane 1, 200 pg; lane 2, 20 pg; lane 3, 2 pg; lane 4, 0.2 pg; lane 5, 0.02 pg; and lane 6, 0.002 pg); lane 7, reverse transcriptase–negative control. C, Lane 0 shows DNA mass ladder; lanes 1 to 6, serial dilutions of NCX RNA internal standard (lane 1, 300 pg; lane 2, 30 pg; lane 3, 3 pg; lane 4, 0.3 pg; lane 5, 0.03 pg; and lane 6, 0.003 pg); lane 7, reverse transcriptase–negative control. Lower bands correspond to channel mRNA products, upper bands to internal standards. The results shown were from 1 control and 1 P42 heart per group. Similar results were obtained in 5 P0 and 5 P42 dogs per construct.

Western Blot Analysis of Changes in Kv4.3 and Na^+ Channel Membrane Protein Expression

Figure 7 (top) shows representative bands from a gel on which Na^+ channel protein was studied. The bands were less intense in the P42 dog hearts. Incubation with the Na^+ channel antigen against which the antibody was raised (supplied by Alomone) resulted in the disappearance of the 220-kDa I_{Na} band (last lane), without altering the lower-molecular-weight marker band lower on the gel. Similar results were obtained in 5 P42 and 7 P0 hearts, with an overall 46.5% reduction in I_{Na} protein in P42 hearts ($P<0.0001$). Figure 7 (middle) shows bands of the expected molecular weight (72 kDa) identified by the anti-Kv4.3 antibodies in a typical gel. Two lanes show Kv4.3 bands from 2 control dog hearts and 2 lanes that were obtained with tissue from P42 hearts. The bands in P42 dogs were consistently of lesser

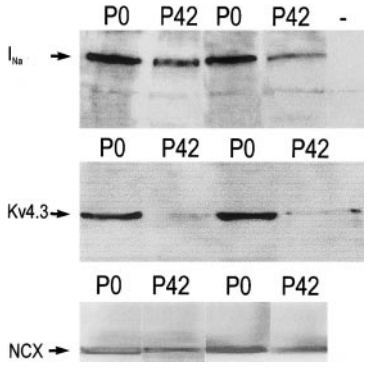

Figure 7. Western blots of membrane protein with an I_{Na} (top), a Kv4.3 (middle), and an NCX (bottom) antibody. Results are shown for 2 hearts per group for each protein.

density compared with bands from sham (P0) dogs, and showed an average 71.6% reduction in Kv4.3 band intensity compared with P0 hearts (n=5 for each, $P<0.001$). Figure 7 (bottom) shows bands corresponding to NCX (MW, 120 kDa), which had the same intensity in P0 and P42 hearts. For 5 hearts in each group, the density in P42 hearts averaged 103% of that in control hearts (P=NS). The marker bands used to confirm equal loading were of very similar density (eg, in the Kv4.3 experiments, their density in P42 hearts averaged 99.8% of the density in P0 hearts; in I_{Na} experiments their density in P42 hearts averaged 100.8% of P0 hearts).

Discussion

We have found that atrial tachycardia reduces the mRNA concentrations of several cardiac ion channels while leaving others unaffected. The ion channels for which mRNA concentrations are altered by rapid atrial pacing are the same channels (I_{Ca}, I_{to}, and I_{Na}) that show reduced function in rapidly paced dogs. In addition, Western blot studies confirmed reductions for P42 dogs in the membrane protein concentrations of Kv4.3 (by 71.6%) and I_{Na} (46.5%) that were quite similar to the reductions in corresponding mRNA concentration (by 74% and 42% in Kv4.3 and I_{Na}, respectively) in P42 dogs. These findings suggest that reduced message levels are responsible for the changes in ion current density that characterize the electrophysiological alterations by which AF leads to its own perpetuation.

Relations Between mRNA Concentrations and Changes in Current Density

The results described above show qualitatively that decreases in mRNA concentration are observed only for currents with a density that changes in paced dogs; for currents (I_{K1} and I_{Kr}) for which function remains unaltered by atrial tachycardia, mRNA concentrations remain stable. To relate quantitatively the mRNA concentrations we measured to physiological changes in current density, we compared changes in mRNA concentration measured in the present study with alterations in current density that we previously recorded in each group of dogs.[10,11] Both functional and molecular data were obtained from tissues in the same right atrial region, the pectinate muscles. Figure 8 shows mean values of mRNA

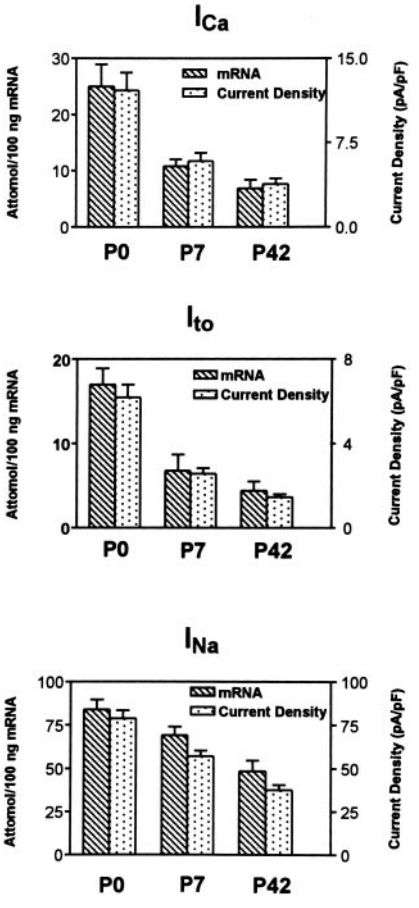

Figure 8. Changes in mRNA concentrations and densities of the corresponding ionic current in each group of dogs. Currents were measured in 25 cells from 5 hearts for each group of dogs for I_{Ca} and I_{to} (Reference [10]), and 28 cells (5 hearts), 59 cells (6 hearts), and 43 cells (6 hearts) for I_{Na} of P0, P7, and P42 dogs, respectively (Reference [11]). Results are mean±SEM for both mRNA concentration and current density.

concentration (measured separately for 5 hearts for each group or construct) and mean densities of the corresponding ionic current (current for I_{Ca} and I_{to} was measured in 25 cells per group; for I_{Na}, 28, 59, and 63 cells were measured in the P0, P7, and P42 groups, respectively). I_{to} was measured with a voltage step from −50 to +20 mV, I_{Ca} was measured with a voltage step from −50 to +10 mV, and I_{Na} was measured with a voltage step from −140 to −40 mV. A close correspondence exists between ion current and mRNA changes. In terms of percentage changes, I_{Ca} mRNA concentrations were reduced by 57% and 72% after 7 and 42 days of pacing, respectively, and I_{Ca} density was reduced by 52% and 69%, respectively, after corresponding pacing periods. I_{to} mRNA concentrations were reduced by 59% and 77% in P7 and P42 dogs, respectively, and the corresponding figures for I_{to} density were 61% and 74%, respectively. For I_{Na}, the reductions in mRNA concentration were 18% and 42% after 7 and 42 days of pacing, respectively, compared with 28% and 52%, respectively, for current density. These results support the notion that alterations in channel α subunit mRNA level resulted in corresponding changes in ion current density.

Alterations in Ion Channel Gene Expression in Experimental Models of Heart Disease

A variety of changes in ion channel gene expression have been observed in animal models of heart disease, primarily at the ventricular level. Matsubara et al[25] noted decreased Kv1.5 mRNA expression and increased Kv1.4 mRNA in rat models of ventricular hypertrophy, with a normalization of gene expression after treatment. Gidh-Jain et al[26] showed a reemergence of fetal pattern L-type Ca^{2+} current mRNA in noninfarcted zones of rats 21 days after myocardial infarction. Subsequent work from the same group showed decreases in mRNA content of 3 K^+ channel genes, Kv1.4, Kv2.1, and Kv4.2, without changes in Kv1.2 or Kv1.5 in the same model.[27] Downregulation of cardiac mRNA encoding the α_1 subunit of I_{Ca} has been noted in patients with end-stage heart failure.[28]

Our observations constitute the first detailed study of changes in ion channel gene expression in experimental models of atrial electrical remodeling due to atrial tachycardia. Because the changes that we observed parallel ion channel abnormalities that account for action potential changes that underlie refractoriness alterations caused by remodeling,[10] they are likely to be of pathophysiological significance.[7]

The regulatory mechanisms that cause the changes in ion channel mRNA concentration that we observed are a subject of great potential interest. We attempted to perform nuclear runoff assays to evaluate changes in transcription rate; however, canine atrial tissue has a relatively small mass, and the largest number of nuclei we were able to isolate ($<10^6$) was insufficient to perform runoff studies. A variety of hormones and neurotransmitter transducers, including thyroid hormone, glucocorticoids, and cAMP, can regulate ion channel expression.[29–32] Autonomic neurotransmitters do not appear to be involved in the phenotypic changes caused by atrial tachycardia,[9] but the potential importance of other endogenous bioactive substances has not been assessed. Cellular Ca^{2+} loading that results from increased action potential frequencies is an attractive possibility because I_{Ca} downregulation could serve an important protective function against Ca^{2+} overload. Evidence for Ca^{2+} overload has been shown early in the rapid-pacing AF model.[33] Ca^{2+} antagonists appear to prevent AF-induced remodeling,[34] and increased cytosolic Ca^{2+} can downregulate mRNA encoding cardiac Na^+ channels.[35] On the other hand, incubation of quiescent rat ventricular myocytes in increased extracellular [Ca^{2+}] solutions increases I_{Ca},[36] and varying results have been obtained in studies of I_{Ca} in ventricles from dogs subjected to rapid ventricular pacing: both a significant decrease[37] and no change[38] have been reported.

Comparison With Previous Observations of Molecular Changes Related to Electrophysiological Abnormalities in AF

We applied competitive RT-PCR, the most sensitive and quantitative method presently available for studying genes expressed at a low level,[39,40] to quantify changes in ion channel expression in a dog model of AF. There is relatively little information available regarding the molecular changes occurring in AF. Van Wagoner et al[41] have reported that atrial myocytes from patients with chronic AF have a reduced density of sustained outward current at the end of a depolarizing pulse, which suggests a reduced density of the ultrarapid delayed rectifier, I_{Kur},[42] and have shown that protein levels of Kv1.5, the α subunit that carries I_{Kur},[42,43] are reduced. Expression of Kv2.1 was not altered, and expression of other K^+, Na^+, and Ca^{2+} channels was not determined. Preliminary data suggest that the density of I_{Ca} in atrial cells from patients with AF is reduced,[44] in agreement with our findings, but biochemical analyses have not been reported. Contradictory findings have been published regarding changes in gap junction protein expression during AF.[45,46] A preliminary communication points to a 36% reduction of mRNA levels of CIR, a component of I_{KACh}, in patients with AF,[47] although it is unclear whether there is a corresponding functional change. An intriguing recent report identifies a genetic locus for a familial form of AF.[48] More precise identification of the gene and its protein product promises to provide exciting insights into the molecular pathophysiology of AF.

Potential Relevance to AF Mechanisms

Changes in atrial refractoriness are ubiquitous in tachycardia-related animal models of AF,[7,9,13] and resemble abnormalities in patients susceptible to AF.[50,51] Action potential duration changes caused by I_{Ca} downregulation account largely for refractoriness changes associated with AF.[10] I_{Ca} reductions could be due to a variety of mechanisms, including decreased production of the channel, changed functional properties of the channel, and altered regulation by guanine nucleotide binding proteins coupled to receptors for endogenous ligands. The voltage and time dependence of I_{Ca} is unaltered, which argues against changes in functional channel properties.[10] In this article, we show that the development of a substrate for sustained AF is associated with decreased levels of mRNA encoding the α subunit of I_{Ca} and that changes in mRNA levels are strongly correlated with alterations in I_{Ca} density. These observations suggest that decreased levels of mRNA encoding the pore-containing α subunit of I_{Ca} lead to decreased channel production and thereby reduce macroscopic current. Several groups have noted prolongations in atrial conduction time, implying slowed atrial conduction, in experimental animals[13,52] and patients[53,54] with AF. Downregulation of I_{Na} caused by a reduction in mRNA levels encoding the I_{Na} α subunit could explain these findings. Together, the changes in atrial refractoriness and conduction are potentially important for explaining how rapid atrial activation promotes the perpetuation of AF.[12]

Potential Limitations

Whereas transcriptional regulation is an important controller of phenotypic expression, the concentration of ion channel mRNA does not always correspond to the expression of the protein or functional channel for which the gene encodes.[24,55,56] It is significant that mRNA concentration changes for I_{to}, I_{Na}, and I_{Ca} in the present study correspond closely to changes in macroscopic current measured previously in our laboratory from identical experimental prepara-

tions. Furthermore, we were able to confirm with the Western blot method that membrane protein concentrations of Kv4.3 and I_{Na} were altered by rapid pacing in a fashion quantitatively very similar to those of corresponding mRNA and macroscopic current. Because of technical limitations, we were unable to assay Ca^{2+} channel proteins by Western blot; however, in a recent study of radioligand binding to dihydropyridine and adrenergic receptors, we found a significant decrease in dihydropyridine receptors in dogs subjected to rapid atrial pacing.[57] This observation suggests that, as for I_{to} and I_{Na}, atrial electrical remodeling reduces I_{Ca} by decreasing the number of L-type Ca^{2+} channels. Although our findings point to transcriptional regulation as the mechanism of changes in ionic current expression, they do not exclude other types of changes (eg, in protein turnover, posttranscriptional modification and functional regulation).

Conclusions

Previous work has shown that alterations in the density of I_{Ca}, I_{Na}, and I_{to} are important in a dog model of sustained AF that shows many electrophysiological features similar to those described in patients with AF. We have found downregulation of messenger RNA concentrations for these channels that parallels quantitatively changes in current density and (for I_{to} and I_{Na}) changes in membrane concentration of the channel α subunit protein. These findings provide a potential molecular mechanism for the electrical remodeling that is both caused by and promotes the persistence of AF and provides an example of how a physiological perturbation can cause changes in gene expression that promote its own perpetuation.

Acknowledgments

This study was supported by the Medical Research Council of Canada, the Heart and Stroke Foundation of Quebec, and the Fonds de Recherche de l'Institut de Cardiologie de Montréal. Lixia Yue is a research student of the Heart and Stroke Foundation of Canada, Dr Gaspo is a Medical Research Council of Canada/PMAC postdoctoral fellow, and Dr Wang is a Heart and Stroke Foundation of Canada research scholar. The authors thank Xiaofan Yang and Maria Kotsiopriftis for expert technical assistance, Dr Jeanne Nerbonne (Washington University, St Louis, Mo) for supplying us with polyclonal Kv4.3 antibody, and Luce Bégin for secretarial help.

References

1. Semenza GL. Transcriptional regulation of gene expression: mechanisms and pathophysiology. *Hum Mutat*. 1994;3:180–199.
2. Moalic JM, Charlemagne D, Mansier P, Chevalier B, Swynghedauw B. Cardiac hypertrophy and failure—a disease of adaptation: modifications in membrane proteins provide a molecular basis for arrhythmogenicity. *Circulation*. 1993;87(suppl IV):IV-21–IV-26.
3. Shalak TC, Price RJ. The role of mechanical stresses in microvascular remodeling. *Microcirculation*. 1996;3:143–165.
4. Simonian NA, Hyman BT. Functional alterations in neural circuits in Alzheimer's disease. *Neurobiol Aging*. 1995;16:305–309.
5. Waktare JE, Camm AJ. Atrial fibrillation begets trouble. *Heart*. 1997;77:393–394.
6. Nattel S. Newer developments in the management of atrial fibrillation. *Am Heart J*. 1995;130:1094–1106.
7. Wijffels MCEF, Kirchhof CJHJ, Dorland R, Allessie MA. Atrial fibrillation begets atrial fibrillation: a study in awake chronically instrumented goats. *Circulation*. 1995;92:1954–1968.
8. Tieleman RG, Van Gelder IC, Crijns HJGM, De Kam PJ, Van Den Berg MP, Haaksma J, Van Der Woude HJ, Allessie MA. Early recurrences of atrial fibrillation after electrical cardioversion: a result of fibrillation-induced electrical remodeling of the atria? *J Am Coll Cardiol*. 1998;31:167–173.
9. Wijffels MC, Kirchhof CJ, Dorland, R, Power J, Allessie MA. Electrical remodeling due to atrial fibrillation in chronically instrumented conscious goats: roles of neurohumoral changes, ischemia, atrial stretch, and high rate of electrical activation. *Circulation*. 1997;96:3710–3720.
10. Yue L, Feng J, Gaspo R, Li G-R, Wang Z, Nattel S. Ionic remodeling underlying action potential changes in a canine model of atrial fibrillation. *Circ Res*. 1997;81:512–525.
11. Gaspo R, Bosch RF, Bou-Abboud E, Nattel S. Tachycardia-induced changes in Na^+ current in a chronic dog model of atrial fibrillation. *Circ Res*. 1997;81:1045–1052.
12. Gaspo R, Bosch RF, Talajic M, Nattel S. Functional mechanisms underlying tachycardia-induced sustained atrial fibrillation in a chronic dog model. *Circulation*. 1997;96:4027–4035.
13. Morillo CA, Klein GJ, Jones DL, Guiraudon CM. Chronic rapid atrial pacing: structural, functional, and electrophysiological characteristics of a new model of sustained atrial fibrillation. *Circulation*. 1995;91:1588–1595.
14. Biel M, Ruth P, Bosse E, Hullin R, Stühmer W, Flockerzi V, Hofmann F. Primary structure and functional expression of a high voltage activated calcium channel from rabbit lung. *FEBS Lett*. 1990;269:409–412.
15. Klöckner U, Mikala G, Eisfeld J, Iles DE, Strobeck M, Mershon JL, Schwartz A, Varadi G. Properties of three COOH-terminal splice variants of a human cardiac L-type Ca^{2+}-channel α_1-subunit. *Am J Physiol*. 1997;272:H1372–H1381.
16. Gellens ME, George AL Jr, Chen LQ, Chahine M, Horn R, Barchi RL, Kallen RG. Primary structure and functional expression of the human cardiac tetrodotoxin-insensitive voltage-dependent sodium channel. *Proc Natl Acad Sci U S A*. 1992;89:554–558.
17. Serôdio P, Vega-Saenz de Miera E, Rudy B. Cloning of a novel component of A-type K^+ channels operating at subthreshold potentials with unique expression in heart and brain. *J Neurophysiol*. 1996;75:2174–2179.
18. Dixon JE, Shi W, Wang H-S, McDonald C, Yu H, Wymore RS, Cohen IS, McKinnon D. Role of the Kv4.3 K^+ channel in ventricular muscle: a molecular correlate for the transient outward current. *Circ Res*. 1996;79:659–668.
19. Wible BA, De Biasi M, Majumder K, Taglialatela M, Brown AM. Cloning and functional expression of an inwardly rectifying K^+ channel from human atrium. *Circ Res*. 1995;76:343–350.
20. Trudeau MC, Warmke JW, Ganetzky B, Robertson GA. HERG, a human inward rectifier in the voltage-gated potassium channel family. *Science*. 1995;269:92–95.
21. Sanguinetti MC, Jiang C, Curran ME, Keating MT. A mechanistic link between an inherited and acquired cardiac arrhythmia: HERG encodes the I_{Kr} potassium channel. *Cell*. 1995;81:299–307.
22. Nicoll DA, Longoni S, Philipson KD. Molecular cloning and functional expression of the cardiac sarcolemmal Na^+-Ca^{2+} exchanger. *Science*. 1990;250:562–565.
23. Altschul SF, Gish W, Miller W, Myers EW, Lipman DJ. Basic local alignment search tool. *J Mol Biol*. 1990;215:403–410.
24. Barry DM, Trimmer JS, Merlie JP, Nerbonne JM. Differential expression of voltage-gated K^+ channel subunits in adult rat heart. Relation to functional K^+ channels? *Circ Res*. 1995;77:361–369.
25. Matsubara H, Suzuki J, Inada M. Shaker-related potassium channel, Kv1.4, mRNA regulation in cultured rat heart myocytes and differential expression of Kv1.4 and Kv1.5 genes in myocardial development and hypertrophy. *J Clin Invest*. 1993;92:1659–1666.
26. Gidh-Jain M, Huang B, Jain P, Battula V, El-Sherif N. Reemergence of the fetal pattern of L-type calcium channel gene expression in non infarcted myocardium during left ventricular remodeling. *Biochem Biophys Res Commun*. 1995;216:892–897.
27. Gidh-Jain M, Huang B, Jain P, El-Sherif N. Differential expression of voltage-gated K^+ channel genes in left ventricular remodeled myocardium after experimental myocardial infarction. *Circ Res*. 1996;79:669–675.
28. Takahashi T, Allen PD, Lacro RV, Marks AR, Dennis AR, Schoen FJ, Grossman W, Marsh JD, Izumo S. Expression of dihydropyridine receptor (Ca^{2+} channel) and calsequestrin genes in the myocardium of patients with end-stage heart failure. *J Clin Invest*. 1992;90:927–935.
29. Mori Y, Matsubara H, Folco E, Siegel A, Koren G. The transcription of mammalian voltage-gated potassium channel is regulated by cAMP in a cell-specific manner. *J Biol Chem*. 1993;268:26482–26493.

30. Takimoto K, Levitan ES. Glucocorticoid induction of Kv1.5 K^+ channel gene expression in ventricle of rat heart. *Circ Res*. 1994;75:1006–1013.
31. Levitan ES, Hershman KM, Sherman TG, Takimoto K. Dexamethasone and stress upregulate Kv1.5 K^+ channel gene expression in rat ventricular myocytes. *Neuropharmacology*. 1996;35:1001–1006.
32. Nishiyama A, Kambe F, Kamiya K, Yamaguchi S, Murata Y, Seo H, Toyama J. Effects of thyroid and glucocorticoid hormones on Kv1.5 potassium channel gene expression in the rat left ventricle. *Biochem Biophys Res Commun*. 1997;237:521–526.
33. Goette A, Honeycutt C, Langberg JJ. Electrical remodeling in atrial fibrillation: time course and mechanisms. *Circulation*. 1996;94: 2968–2974.
34. Tieleman RG, De Langen C, Van Gelder IC, de Kam PJ, Grandjean J, Bel KJ, Wijffels MC, Allessie MA, Crijns HJ. Verapamil reduces tachycardia-induced electrical remodeling of the atria. *Circulation*. 1997; 95:1945–1953.
35. Duff HJ, Offord J, West J, Catterall WA. Class I, and IV antiarrhythmic drugs and cytosolic calcium regulate mRNA encoding the sodium channel alpha subunit in rat cardiac muscle. *Mol Pharmacol*. 1992;42: 570–574.
36. Davidoff AJ, Maki TM, Ellingsen O, Marsh JD. Expression of calcium channels in adult cardiac myocytes is regulated by calcium. *J Mol Cell Cardiol*. 1997;29:1791–1803.
37. Mukherjee R, Hewett KW, Spinale FG. Myocyte electrophysiological properties following the development of supraventricular tachycardia-induced cardiomyopathy. *J Mol Cell Cardiol*. 1995;27: 1333–1348.
38. Kaab S, Nuss HB, Chiamvimonvat N, O'Rourke B, Pak PH, Kass DA, Marban E, Tomaselli GF. Ionic mechanism of action potential prolongation in ventricular myocytes from dogs with pacing-induced heart failure. *Circ Res*. 1996;78:262–273.
39. Zhang J, Desai M, Ozanne SE, Doherty C, Hales CN, Byrne CD. Two variants of quantitative reverse transcriptase PCR used to show differential expression of α-, β- and γ-fibrinogen genes in rat liver lobes. *Biochem J*. 1997;321:769–775.
40. Gattei V, Degan M, De Iuliis A, Rossi FM, Aldinucci D, Pinto A. Competitive reverse-transcriptase PCR: a useful alternative to Northern blotting for quantitative estimation of relative abundances of specific mRNAs in precious samples. *Biochem J*. 1997;325:565–567.
41. Van Wagoner DR, Pond AL, McCarthy PM, Trimmer JS, Nerbonne JM. Outward K^+ current densities and Kv1.5 expression are reduced in chronic human atrial fibrillation. *Circ Res*. 1997;80:772–781.
42. Wang Z, Fermini B, Nattel S. Sustained depolarization-induced outward current in human atrial myocytes: evidence for a novel delayed rectifier K^+ current similar to Kv1.5 cloned channel currents. *Circ Res*. 1993;73: 1061–1076.
43. Feng J, Wible B, Li GR, Wang Z, Nattel S. Antisense oligonucleotides directed against Kv1.5 mRNA specifically inhibit ultrarapid delayed rectifier potassium current in cultured adult human atrial myocytes. *Circ Res*. 1997;80:572–579.
44. Van Wagoner DR, Lamorgese M, Kirian P, Cheng Y, Efimov IR, Mazgalev TN, Nerbonne JM. Calcium current density is reduced in atrial myocytes isolated from patients in chronic atrial fibrillation. *Circulation*. 1997;96(suppl I):I-180. Abstract.
45. Elvan A, Huang XD, Pressler ML, Zipes DP. Radiofrequency catheter ablation of the atria eliminates pacing-induced sustained atrial fibrillation and reduces connexin 43 in dogs. *Circulation*. 1997;96:1675–1685.
46. Van der Velden HMW, van Zijverden M, van Kempen MJA, Wijffels MCEF, Groenewegen WA, Allessie MA, Jongsma HJ. Abnormal expression of the gap junction protein connexin 40 during chronic atrial fibrillation in the goat. *Circulation*. 1996;94(suppl I):I-593. Abstract.
47. Brundel BJ, Van Gelder IC, Henning RH, Deelman LE, Tuinenburg AE, Van Gilst WH, Crijns HJ. Decreased levels of IKACh mRNA in patients with chronic atrial fibrillation but no changes in the sarcoplasmic reticulum calcium ATPase and phospholamban. *J Am Coll Cardiol*. 1997;29(suppl A):122A. Abstract.
48. Brugada R, Tapscott T, Czernuszewicz GZ, Marian AJ, Iglesias A, Mont L, Brugada J, Girona J, Domingo A, Bachinski LL, Roberts R. Identification of a genetic locus for familial atrial fibrillation. *N Engl J Med*. 1997;336:905–911.
49. Singer D, Biel M, Lotan I, Flockerzi V, Hofmann F, Dascal N. The roles of the subunits in the function of the calcium channel. *Science*. 1991; 253:1553–1557.
50. Attuel P, Childers R, Cauchemez B, Poveda J, Mugica J, Coumel P. Failure in the rate adaptation of the atrial refractory period: its relationship to vulnerability. *Int J Cardiol*. 1982;2:179–197.
51. Boutjdir M, Le Heuzey JY, Lavergne T, Chauvaud S, Guize L, Carpentier A, Peronneau P. Inhomogeneity of cellular refractoriness in human atrium: factor of arrhythmia? *PACE Pacing Clin Electrophysiol*. 1986; 9(part II):II-1095–II-1100.
52. Elvan A, Wylie K, Zipes DP. Pacing-induced chronic atrial fibrillation impairs sinus node function in dogs: electrophysiological remodeling. *Circulation*. 1996;94:2953–2960.
53. Cosio FG, Palacios J, Vidam JM, Cocina EG, Gomez-Sanchez A, Tamargo L. Electrophysiologic studies in atrial fibrillation: slow conduction of premature impulses: a possible manifestation of the background for reentry. *Am J Cardiol*. 1983;51:122–130.
54. Kumagai K, Akimitsu S, Kawahira K, Kawanami F, Yamanouchi Y, Hiroki T, Arakawa K. Electrophysiological properties in chronic lone atrial fibrillation. *Circulation*. 1991;84:1662–1668.
55. Dixon JE, McKinnon D. Quantitative analysis of potassium channel mRNA expression in atrial and ventricular muscle of rats. *Circ Res*. 1994;75:252–260.
56. Xu H, Dixon JE, Barry DM, Trimmer JS, Merlie JP, McKinnon D, Nerbonne JM. Developmental analysis reveals mismatches in the expression of K^+ channel α subunits and voltage-gated K^+ channel currents in rat ventricular myocytes. *J Gen Physiol*. 1996;108:405–419.
57. Gaspo R, Sun H, Fareh S, Levi M, Yue L, Allen BG, Hebert TE, Nattel S. Dihydropyridine and β-adrenergic receptor binding in dogs with tachycardia-induced atrial fibrillation. *Cardiovasc Res*. In press.

Molecular Mechanisms Underlying Ionic Remodeling in a Dog Model of Atrial Fibrillation

Lixia Yue, Peter Melnyk, Rania Gaspo, Zhiguo Wang and Stanley Nattel

Circ Res. 1999;84:776-784
doi: 10.1161/01.RES.84.7.776
Circulation Research is published by the American Heart Association, 7272 Greenville Avenue, Dallas, TX 75231

Print ISSN: 0009-7330. Online ISSN: 1524-4571